Optics Letters

Compact chirped-pulse amplification systems based on highly Tm^{3+}-doped germanate fiber

Zhengqi Ren,[1] Fedia ben Slimen,[1,*] Joris Lousteau,[2] Nicholas White,[1] Yongmin Jung,[1] Jonathan H. V. Price,[1] David J. Richardson,[1] and Francesco Poletti[1]

[1]Optoelectronics Research Centre, University of Southampton, Southampton SO17 1BJ, UK
[2]Department of Chemistry and Materials Engineering (CMIC), Politecnico di Milano, Via Mancinelli, 7, 20131 Milano, Italy
*Corresponding author: f.ben-slimen@soton.ac.uk

Received 11 February 2021; revised 2 April 2021; accepted 19 April 2021; posted 21 April 2021 (Doc. ID 422336); published 17 June 2021

We report the fabrication of a dual cladding large mode area thulium-doped germanate fiber (TDGF). The fiber has a core diameter of 20 μm, a high Tm^{3+} ion concentration of 3 cm^3 × 10^{20}/cm^3, and a hexagonal inner cladding to enhance pump absorption when cladding-pumped. Using a short fiber length, we demonstrate a compact 300 fs chirped-pulse amplification system operating at 1925 nm, investigating both core- and cladding-pumped implementations. By cladding pumping a 65 cm long fiber we produced an average power of 14.1 W (limited by thermally induced damage) and a peak power of 2.17 MW at a pulse repetition rate of 15.7 MHz. Core pumping a 19 cm length of TDGF produced 2.3 W of average-power and 16 MW peak-power pulses at 0.39 MHz. The performance is already comparable to the state-of-the-art success achieved with flexible silica fibers. Considering the rapid improvements in glass quality and the scope for further increasing the doping concentration, this fiber type holds great potential for pulsed fiber lasers in the 1.5–3 μm wavelength region.

Published by The Optical Society under the terms of the Creative Commons Attribution 4.0 License. Further distribution of this work must maintain attribution to the author(s) and the published article's title, journal citation, and DOI.

https://doi.org/10.1364/OL.422336

High-power ultra-short pulse laser sources in the 2 μm wavelength range are gaining more and more attention for use in applications, including free-space optical communications, sensing, material processing, and mid-IR generation [1]. They are also proving promising for fundamental research in fields such as high-harmonic generation [2] and laser-driven electron acceleration [3]. Thulium (Tm)-doped photonic crystal fibers [4,5] have been used to achieve the highest pulse energies (millijoule level) and peak/average powers (gigawatt/kilowatt) to date. However, many important practical applications, including material processing and power scaling of mid-IR light generation, do not require such levels of performance and, consequently, there is appreciable commercial interest in more practical, compact sources based on more conventional flexible fiber technology with relatively simple physical configurations.

The current performance records for compact, high-power Tm-based UV-fast fiber laser systems have been set by using conventional silica fibers. For example, Wan *et al.* demonstrated a chirped-pulse amplification (CPA) system, which achieved an output average power of 32 W by using 650 meters of fiber stretcher and 4.5 m large mode area (LMA) fiber [6]. The generation of 0.15 μJ energy, 0.5 MW peak power, 256 fs pulses was demonstrated by Haxsen *et al.* using a 2.8 m LMA fiber [7]. By increasing the stretched pulse duration to 160 ps, Sims *et al.* used a 3.3 m LMA fiber to achieve 1 μJ, 3 MW peak-power pulses [8]. Hoogland and Holzwarth demonstrated a compact CPA system, which generated pulses with 1 MW peak power and 371 fs duration with a 3.4 m LMA fiber amplifier [9]. All these silica fiber-based results required active fiber lengths above 1 m, which resulted in limited pulse-energy/peak-power scaling due to the appearance of detrimental nonlinear effects, including modulation instability and spectral broadening from self-phase modulation.

Although silica glass is clearly both the dominant and most technologically developed host material for fiber lasers, due largely to its combination of favorable mechanical and glass-drawing characteristics, it has low rare-earth ion solubility, which limits the scope for reducing the lengths of active fiber in lasers and amplifiers. The maximum Tm^{3+} doping concentration in pure-silica fiber is 10^{18}–10^{19} ions/cm^3 [10]. Higher doping levels (10^{20} ions/cm^3) can be realized through the addition of co-dopants such as aluminum or phosphorous [11], but these substantially increase the core refractive index relative to a pure-silica cladding, so cores with a surrounding pedestal structure are required to create the low-index step needed in LMA designs. The need for this refractive index pedestal makes fabrication more complex. In contrast, heavy metal oxide glasses such as germanate and fluoride have much higher Tm^{3+} solubility with concentrations of 10^{21} ions/cm^3 being readily achievable without the addition of co-dopants. The resulting promise of shorter device lengths should reduce the impact of detrimental nonlinearities in pulsed laser systems. Germanate and fluoride glasses systems can be easily and directly index-matched to pure cladding glasses, enabling simplified LMA step-index fiber design and fabrication. Here we focus on germanate glass, which has a nonlinear index approximately twice that of pure silica, so

a reduction in device length by approximately that the factor is required to compete with silica devices.

The other concern with silica glass is its high phonon energy of ~1100 cm^{-1}, which results in fast multiphonon relaxation in the mid-IR, where it becomes opaque and can lead to a low cross-relaxation rate and thus reduction in quantum efficiency when pumping thulium at 793 nm [12–14]. In contrast, germanate glasses [15] possess a 25% lower phonon energy of ~845 cm^{-1} [16]. Hence, germanate fiber is attractive for laser transitions at long wavelengths that would not be useable in a silica glass host fiber. The outstanding challenges for realizing practical germanate fibers are in the fabrication of a glass with the lowest possible levels of impurities and in the preparation of a preform and fiber that do not suffer from crystallization so as to minimize propagation losses and achieve optimal laser performance.

Some good laser results with germanate fibers have already been achieved. Wen *et al.* demonstrated a single-frequency fiber laser at 1.95 μm using just 1.6 cm of a highly Tm-doped (7.6×10^{20} ions/cm^3) barium gallo-germanate single-mode (SM) fiber, but with a low output power (35 mW) and even moving to a length of 10 cm for multi-longitudinal-mode laser operation, only 165 mW of output power was achieved with a moderate slope efficiency (17%) [16]. Fang *et al.* demonstrated a nanosecond-pulsed 2 μm single-frequency master oscillator power amplifier using 41 cm of large core (30 μm) thulium-doped germanate fiber (TDGF), obtaining a record output average power of 16 W and peak power of 73 kW [17]. However, their amplification slope efficiency of 17% was again low due to a high background loss of 5 dB/m in their fiber.

In this Letter, we demonstrate a TDGF with high dopant concentration, low background loss, and a hexagonal cladding structure which enables efficient high-power cladding pumping. To highlight the opportunities this presents for laser development, we incorporated 65 cm of fiber, cladding pumped, in a compact, high average- and peak-power CPA system operating at 1925 nm, achieving 310 fs compressed pulses at an average power of 14.1 W and a peak power of 2.17 MW at a repetition rate of 15.7 MHz. By core pumping 19 cm of the same fiber and reducing the pulse repetition rate to 0.39 MHz, we generated 290 fs pulses at average power of 2.3 W and peak power of 16 MW.

For the TDGF development, both the germanate core glass (Ge-01) and cladding glass (Ge-02) were made in house, using the melt-quenching technique from the chemical composition of $58GeO_2 - 15PbO - 13ZnO - 4Nb_2O_5 - 7Na_2O - 1.5SiO_2 - 1.5Al_2O_3$ [18].

The combination provided the low-refractive-index contrast necessary for SM LMA fiber operation and compatibility in terms of the thermos-mechanical properties needed for successful fiber drawing. We achieved a high Tm^{3+} concentration of 3×10^{20} ions/cm^3, a large core diameter of 20 μm, and a low numerical aperture (NA = 0.07) which, together, enabled robust SM operation.

The fabrication process for the germanate glasses and TDGF were similar to the process described in our report of a TDGF with a circular inner cladding [18]. The Ge-01 cane and Ge-02 hexagonal glass tube were co-drawn into an optical fiber using a rod-in-tube technique (Fig. 1 left). The fiber core and cladding diameters were 20 ± 0.5 and 126 ± 1 μm (across two opposite angles), respectively.

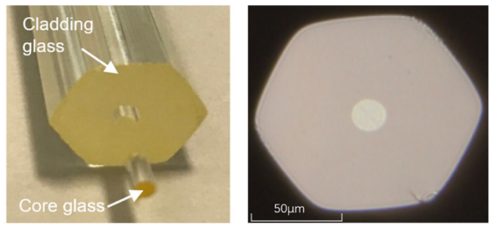

Fig. 1. (Left) Cross-sectional view of the extruded hexagonal inner cladding with the core rod extending outwards from the front face. (Right) Optical microscope image of the fabricated Tm-doped germanate LMA SM fiber.

As shown in Fig. 1 (right), there are no signs of residual stresses or bubbles at the interface between the core and cladding, which demonstrates the excellent quality of the drawing process. A UV curable low-index acrylate polymer coating around the hexagonal cladding was added to provide mechanical protection and to allow the fiber to be cladding pumped by confining the pump power in the inner cladding. The fiber propagation loss was measured to be ~1 dB/m at 980 nm using the cutback method, matching the lowest loss achieved for germanate glass fiber we reported earlier [17] and confirming the good reproducibility we have achieved in fabricating the high-quality germanate glass material, and the excellent control we have of the fiber fabrication process.

The cladding-pumped CPA system is illustrated schematically in Fig. 2. It composes a fiber oscillator, fiber stretcher, two amplifier stages, and a bulk grating-based compressor. The dissipative soliton fiber oscillator has been described previously [19], and it provides chirped laser output pulses with a width of 25 ps, at a central wavelength of 1925 nm (39 nm bandwidth) at a repetition rate of 15.7 MHz. The average-power output power was 40 mW (corresponding to a pulse peak power of 102 W). The pulses were then attenuated to 3 mW average power to minimize nonlinearity in the stretcher, which consisted of 58 m of UHNA7 (Nufern) and 25 m of UHNA4 (Nufern) fibers. This combination of fiber lengths was chosen to cancel the overall third-order dispersion and to produce stretched pulses with duration of 140 ps [20]. These were amplified to an average power of 150 mW in a 1.5 m Tm-doped silica fiber (OFS, TmDF200) which was backward core-pumped with power of 400 mW at 1560 nm so as to minimize the effective nonlinear length.

To obtain the single polarization required for our transmission grating-based compressor, we used a polarization-maintaining (PM) fast-axis blocking isolator preceded by an in-line polarization controller (FIBERPRO PC1100) between the pre- and power-amplifier stages. Due to slight depolarization

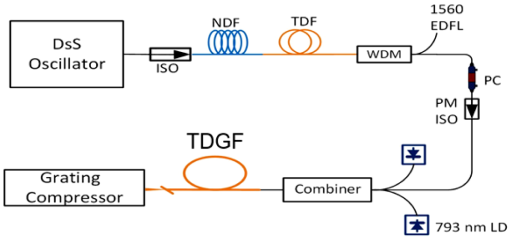

Fig. 2. Schematic diagram of the CPA system. DsS, dissipative soliton; NDF, normal dispersion fiber; WDM, wavelength-division multiplexer; PC, polarization controller; EDFL–Er, doped fiber laser.

in the fiber stretcher, the power reduced from 150 to 110 mW, even after precise adjustment of the PC. The final power amplifier composed 65 cm of TDGF, which was cladding-pumped by two 30 W multimode-diodes (BWT) at 793 nm through a fiberized 130 μm cladding-diameter silica fiber-based combiner (Lightcomm) with a 10 μm core throughput. The cladding absorption was 20 dB/m at 793 nm, and the TDGF length was chosen to obtain a suitably centered spectral gain profile and a good amplifier efficiency. The mode field diameter of the TDGF at 1925 nm was 22.6 μm. The measured splicing losses between the TDGF and the combiner fiber were <1.2 dB (due to the mode field diameter mismatch) and 0.2 dB, respectively, for the core and cladding.

An offset-arc splicing technique (i.e., offsetting the arc position from the splicing location) was used, because the germanate fiber has a lower melting temperature than silica glass [21]. The splice was re-coated with low-index polymer, the TDGF was mounted onto a water-cooled plate, and graphite sheets were applied to assist in the overall thermal management. Although the available pump power was 60 W, the TDGF fiber damaged (inside the fiber and close to the input facet) at pump powers above 53 W. (We observed this on five separate occasions at the ∼50 W power level.) We also observed the same effect when the pulsed seed was replaced with a cw-seed laser. In order to analyze the heat load of the TDGF, the temperature distribution of our fiber (fiber length = 65 cm) was simulated using COMSOL Multiphysics at cladding pump power of 50 W. The fiber coating temperature reaches almost 100°C. Consequently, we conclude that the damage we observed experimentally was due to thermal damage. We estimate that it may be possible to further increase the pump power by a factor of 4 or so based on the improved cooling arrangements and metal coating approach described in [22], but as of yet we have not investigated this. The maximum amplifier output was consequently limited to 20 W, and the launched pump slope efficiency was 38.7% [see Fig. 3(a)], well above the 32% we achieved using a commercial Tm-doped silica fiber in earlier work in the same basic setup [19]. No degradation in output power was observed over the >20 h of total use of our CPA system, implying that photodarkening is not an issue in our fibers. To validate this more carefully, we undertook a more systematic experiment in which we incorporated a length of fresh fiber in our amplifier and seeded it with cw-laser light at 1953 nm. The amplifier was operated at our maximum pump power of 50 W, and the amplified output power was measured every 30 s for a period of 6 h from the first turn on. As shown in Fig. 3(b), no degradation in output power was observed over the duration of our experiment confirming that photodarkening is not an issue on this fiber in

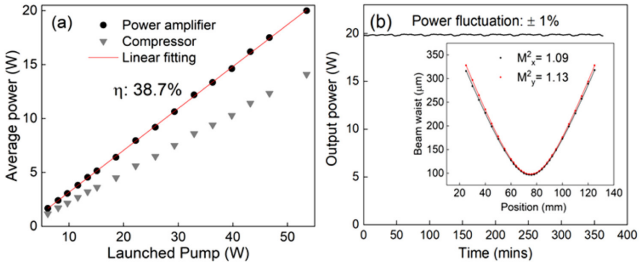

Fig. 3. (a) Measured average output power after the cladding-pumped power amplifier and compressor gratings versus launched pump power. (b) Long-term stability test at the highest output power and the measured M^2 value ($M^2 \sim 1.1$).

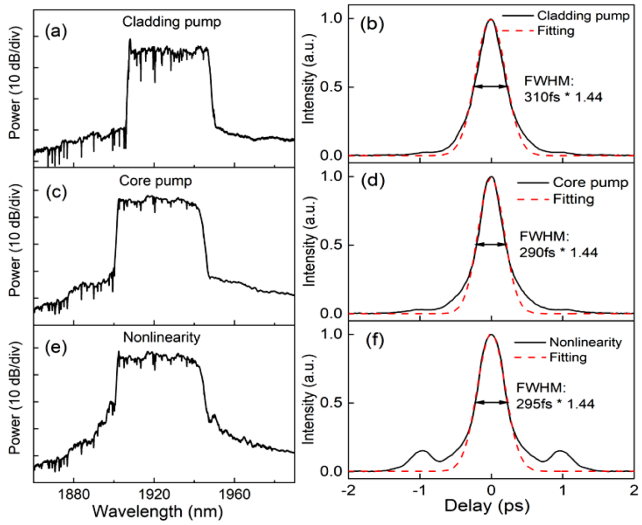

Fig. 4. Output spectra from the power amplifier and autocorrelation traces after the compressor. (a) and (c) Spectra at the maximum amplifier output power of 20 and 3.2 W for cladding pumping and core pumping, respectively. (b) and (d) Autocorrelation trace at the maximum output power of 14.1 and 2.3 W after the compressor for cladding pumping and core pumping, respectively. (e) Spectrum at a higher amplifier output power of 3.6 W for core pumping. (f) Autocorrelation trace at an output power of 2.55 W after the compressor for core pumping illustrating the deleterious impact of nonlinearity in the final stage amplifier.

agreement with our CPA system observations. The output beam quality was also measured at the maximum output power of 14.1 W (after the compressor), and the high beam quality factor ($M^2 \sim 1.1$) was confirmed. The output spectrum is shown in Fig. 4(a).

The pulses were then recompressed using a pair of fused silica transmission gratings (Ibsen Photonics A/S) with a single-pass transmission efficiency of 94% in the 1900–2100 nm range. The polarization of the pulses incident to the gratings was controlled using bulk wave plates at the fiber output. (A maximum incident PER of 16 dB was achieved.) The overall double-pass compressor throughput was 14.1 W (70.5% measured efficiency). With an appropriate grating separation, a minimum compressed pulse duration of 310 fs was achieved as measured with a SHG autocorrelator (APE pulseCheck) [see Fig. 4(b)]. The estimated time bandwidth product (TBP) of 0.98 is 2.2 times the transform-limited value for a Gaussian pulse (0.44), but close to that of a transform-limited pulse with a rectangular spectrum (0.88).

We calculated the Fourier transform of the spectrum and estimated that 75% of the energy was in the main peak yielding a peak-power estimate of 2.17 MW. Note that the atmospheric gas absorption lines clearly observable in the spectra in Fig. 4 originate from free-space propagation in the air within the compressor (path length = 2.4 m) and during measurement in the OSA (internal path length approximately 2.8 m). It has previously been demonstrated that such gas absorption lines can degrade the temporal quality of compressed pulses, resulting in the formation of extended pulse tails extending over a time frame of several picoseconds [23]. By calculating the Fourier transform of the measured pulse spectrum, including the air absorption lines and with those artificially removed numerically,

we estimate that only 2% of the pulse energy is shed into low-level pulse tails in our experiments due to absorption in air. As shown in Fig. 3(b), the spatial mode out of the compressor was measured to have M_x^2 and M_y^2 of 1.09 and 1.13, respectively, indicating close to pure SM operation and confirming that the desired fundamental mode guidance was achieved in the TDGF. We next investigated core pumping a shorter length of TDGF (19 cm) in the power amplifier for pulse-energy and peak-power scaling. A fiber-coupled polarization dependent acousto-optic modulator was inserted after the pre-amplifier to reduce the repetition rate from 15.7 to 0.39 MHz. A 30 cm of PM Tm-doped fiber with a core diameter of 10 μm (Nufern) was core-pumped at 1560 nm and added as an extra pre-amplifier to boost the power into the final amplifier from 0.8 to 40 mW.

The 19 cm TDGF final amplifier was core-pumped via a 1565 nm EDFL pump laser (SPI Lasers) having a maximum power of 10 W through a PM-WDM coupler (Lightcomm). The core splicing loss between the TDGF and pigtail fiber of the silica fiber based-PM-WDM was similar to that of the cladding-pumped case (<1.2 dB). Figure 4(c) shows the signal spectrum at the maximum average output power of 3.2 W for an incident pump power of 9 W (measured immediately after the WDM), this is the highest output power achieved in germanate fibers using in-band core pumping (corresponding to a slope efficiency with respect to incident pump power of 36%). Accounting for a careful cutback measured splice loss of 1.2 dB for the launched pump in the core, the slope efficiency with respect to absorbed pump power was 48%, which is comparable to the value we reported previously [19]. The corresponding autocorrelation trace of the compressed pulse is shown in Fig. 4(d) and shows a pulse duration of 290 fs. The TBP of 0.94 is similar to the cladding-pumped result. We calculated that 80% of the energy was in the body of the pulse; thus, at a recompressed average power of 2.3 W, the pulse energy was estimated to be 4.7 μJ, and the peak power was estimated to be 16 MW. Excellent spatial mode quality was evidenced by the M_x^2 and M_y^2 values of 1.09 and 1.11, respectively.

The maximum pulse energy was limited in these experiments by the appearance of spectral wings induced by nonlinear effects as shown in Fig. 4(e) (data taken at an incident pump power of 10 W and an amplifier output power of 3.55 W). The corresponding compressed autocorrelation trace shown in Fig. 4(f) indicates the formation of significant satellite pulses.

In conclusion, we have fabricated a highly doped TDGF with a hexagonal inner cladding for an efficient cladding-pumped amplifier. In-house glass melting, preform glass extrusion, and fiber drawing were used to achieve a background loss of just 1 dB/m, matching our earlier result [18]. Cladding pumping of a 65 cm length of TDGF produced pulses with average power of 14.1 W and peak power of 2.17 MW at the output of our CPA system. Core pumping a 19 cm TDGF produced pulses with average power of 2.3 W and a peak power of 16 MW. The results are already comparable with our record peak/average powers from a very similar femtosecond conventional/flexible fiber Tm-doped silica fiber CPA system [19], which confirms that the highly Tm^{3+}-doped germanate glass SM fiber can be an alternative to silica-based fiber for 2 μm high-energy/peak-power pulse generation. Given the rapid ongoing progress in our fiber development processes, this fiber technology should ultimately be capable of achieving higher peak powers and similar or possibly even higher average powers in the future. Thus, the next step in our research is to optimize the fiber fabrication to enable greater power scaling. In parallel, we will explore the possibility of further peak-power scaling by shortening the fiber length with a newly developed LMA germanate glass fiber with higher Tm^{3+} doping concentration (8.5×10^{20} ions/cm^3) for which the luminescence intensity reaches its maximum at 1.8 μm [24].

Funding. Engineering and Physical Sciences Research Council (EP/P012248/1, EP/P027644/1, EP/P030181/1); European Research Council (682724).

Acknowledgment. Z. Ren thanks the China Scholarship Council for financial support of his Ph.D.

Disclosures. The authors declare no conflicts of interest.

Data Availability. Data published in this Letter are available from the University of Southampton repository [25].

REFERENCES

1. Q. Fu, L. Xu, S. Liang, D. P. Shepherd, D. J. Richardson, and S. Alam, IEEE J. Quantum Electron. **24**, 1 (2018).
2. M. P. Arpin, T. Popmintchev, M. Gerrity, B. Zhang, M. Seaberg, D. Popmintchev, M. M. Murnane, and H. C. Kapteyn, Phys. Rev. Lett. **105**, 173901 (2010).
3. E. A. Peralta, K. Soong, R. J. England, E. R. Colby, Z. Wu, B. Montazeri, C. McGuinness, J. McNeur, K. J. Leedle, D. Walz, E. B. Sozer, B. Cowan, B. Schwartz, G. Travish, and R. L. Byer, Nature **503**, 91 (2013).
4. C. Gaida, M. Gebhardt, T. Heuermann, F. Stutzki, C. Jauregui, and J. Limpert, Opt. Lett. **43**, 5853 (2018).
5. C. Gaida, M. Gebhardt, F. Stutzki, C. Jauregui, J. Limpert, and A. Tünnermann, Opt. Lett. **41**, 4130 (2016).
6. P. Wan, L.-M. Yang, and J. Liu, Opt. Express **21**, 21374 (2013).
7. F. Haxsen, D. Wandt, U. Morgner, J. Neumann, and D. Kracht, Opt. Lett. **35**, 2991 (2010).
8. R. A. Sims, P. Kadwani, A. L. Shah, and M. Richardson, Opt. Lett. **38**, 121 (2013).
9. H. Hoogland and R. Holzwarth, Opt. Lett. **40**, 3520 (2015).
10. F. Auzel and P. Goldner, Opt. Mater. **16**, 93 (2001).
11. R. Tumminelli, V. Petit, A. Carter, A. Hemming, N. Simakov, and J. Hob, Proc. SPIE **10512**, 105120M (2018).
12. B. M. Walsh and N. P. Barnes, Appl. Phys. B **78**, 325 (2004).
13. M. Eichhorn and S. D. Jackson, Appl. Phys. B **90**, 35 (2008).
14. S. D. Jackson, Opt. Commun. **230**, 197 (2004).
15. J. Wu, Z. Yao, J. Zong, and S. Jiang, Opt. Lett. **32**, 638 (2007).
16. X. Wen, G. Tang, Q. Yang, X. Chen, Q. Qian, Q. Zhang, and Z. Yang, Sci. Rep. **6**, 20344 (2016).
17. Q. Fang, W. Shi, K. Kieu, E. Petersen, A. Chavez-Pirson, and N. Peyghambarian, Opt. Express **20**, 16410 (2012).
18. F. B. Slimen, S. Chen, J. Lousteau, Y. Jung, N. White, S. Alam, D. J. Richardson, and F. Poletti, Opt. Mater. Express **9**, 4115 (2019).
19. Z. Ren, Q. Fu, L. Xu, J. H. V. Price, S. Alam, and D. J. Richardson, Opt. Express **27**, 36741 (2019).
20. P. Elahi, H. Kalaycioğlu, Ö. Akçaalan, Ç. Şenel, and F. Ö. Ilday, Opt. Lett. **42**, 3808 (2017).
21. R. Thapa, R. R. Gattas, V. Nguyen, G. Chin, D. Gibson, W. Kim, L. B. Shaw, and J. S. Sanghera, Opt. Lett. **40**, 5074 (2015).
22. J. Daniel, N. Simakov, A. Hemming, W. Clarkson, and J. Haub, Opt. Express **24**, 18592 (2016).
23. M. Gebhardt, C. Gaida, F. Stutzki, S. Hädrich, C. Jauregui, J. Limpert, and A. Tünnermann, Opt. Express **23**, 13776 (2015).
24. F. B. Slimen, Z. Ren, A. Ventura, J. G. Hayashi, J. Cimek, N. White, Y. Jung, D. J. Richardson, and F. Poletti, Proc. SPIE **11206**, 1120609 (2019).
25. Z. Ren, F. B. Slimen, J. Lousteau, N. White, Y. Jung, J. H. V. Price, D. J. Richardson, and F. Poletti, "Dataset for: Compact chirped-pulse amplification systems based on highly Tm3+ doped germanate fiber," University of Southampton (2021), https://doi.org/10.5258/SOTON/D1807.

131.175.148.47 on 2024-10-08 03:28:53